



Research on Electromagnetic Driving Robot Fish



Zhu Hongxiu^{1*}, Gao zihang², Liang Pinghua³ and Sang wei⁴

Department of Mechanical and Electronics, China University of Mining and Technology, China

Submission: December 13, 2017; Published: March 14, 2018

*Corresponding author: Zhu Hongxiu, Department of Mechanical and Electronics, China University of Mining and Technology (Beijing), Beijing, 100083, China, Email: zhx@cumbt.edu.cn

Abstract

Based on the actual physical appearance of the tuna and the wave equation derived from observing its swimming locomotion, this paper proposes a new idea on the simulation and modeling of the robot fish and a novel way of thinking on kinetic analysis. The motion law for each joint of the robot fish was first obtained through the discrete fitting method and the motion law was subsequently used as the basis for the robot fish electromagnetic drive control signal. The fluent flow field analysis software was utilized. The meshing of the fluid around the fish body was performed by using the dynamic grid technique. The surface pressure values of the fish body during the steady state forward movement were analyzed, and the values of the driving force of each part of the fish were obtained. It was then determined that the electromagnetic drive caudal fin robot fish was the optimal design. Based on the idea of digital-analog conversion, the drive control signal waveform was digitally discretized, then the C51 single-chip microcomputer and DAC digital-to-analog converter was used for conversion. The OPA544 op amp chip was then used to simulate the amplified output in accordance with the control signal waveform. Electromagnetic coil drive signal with variable frequency and voltage can thus be achieved.

Keywords: Robot fish; Electromagnetic drive; Fluent flow field analysis; Kinetic analysis; Control signal; Swimming experiment

Construction of the Robot Fish Model

Determination of the external physical characteristics of the fish body and the number of joints

A real tuna fish was selected, the total length was measured and the external curve of the fish body was fitted; the following data can be obtained:

Total length $l = 260\text{mm}$

$$R(x) = R_1 \sin(R_2 x) + R_3 (e^{R_4 x} - 1)$$

$$r(x) = r_1 \sin(r_2 x) + r_3 (r_4 x - 1)$$

Where $R(x)$ is the function of the longitudinal fish body curve, $r(x)$ is the function of the transverse fish body curve

$$R_1 \approx 0.1l, R_2 \approx \frac{2\pi}{1.57l}, R_3 \approx 0.00008l, R_4 \approx \frac{2\pi}{0.81l}, r_1 \approx 0.05l, r_2 \approx \frac{2\pi}{1.25l}$$

$$r_3 \approx 0.08l, r_4 \approx \frac{2\pi}{3.14l}$$

In the selection of the number of joints of the robot fish, the higher the number of joints, the higher the degree of fit between the swimming curve and the known fish body wave equation, the closer it is to the real fish-swimming situation. On the other hand, the cumulative error of the series structure and the complexity of the structure should also be considered. Usually the range for the number of robot joints N is 2-10. The number of robot fish joints designed in this paper is $N = 6$.

In the design of the length of each joint, considering that the movement of the fish body is mainly concentrated in the rear half of the fish body, therefore the first half 130 mm of the fish can be viewed as not swinging. Also, according to the actual measurement, it is known that the fish tail length is 47 mm. Based on the joint size parameter optimization design method proposed by Chai Zhikun [1], except for the tail joint, the proportion of the remaining five joints should be 83: 67: 59: 53: 48. The length of each joint after calculation and rounding is: joint 1 is 22mm, joint 2 is 18mm, joint 3 is 16mm, joint 4 is 14mm, joint 5 is 13mm, and the joint 6 (caudal fin) is 47mm long.

Calculation of the mass and moment of inertia of each part

Based on the above geometric parameters of the fish, the mass of the various parts of the fish can be calculated:

$$m(x) = \int_a^b \rho \pi R(x) r(x) dx$$

Where, ρ is the fish density (kg/m^3), which can be approximated as the density of water, a, b are the abscissa values of the starting point and the end of each joint.

During the swimming process of the fish, due to interaction with the surrounding fluid, the fish has a virtual mass. According to Lighthill's "Large-amplitude elongated-body

theory of fish locomotion," the equation for calculation of the virtual mass of the fish body cross-section is [2]:

$$m_a \approx \int_a^b \beta \pi R^2(x) \rho_f dx$$

Where, ρ_f is the fluid density, β is the virtual mass coefficient; when there is no fish fins on the fish cross-section, $\beta = 1$.

As the robot fish cross-section can be regarded as an oval with the long axis of $2R(x)$, the short axis of $2r(x)$, the inertia of each part around the z-axis can be calculated according to the following formula:

$$I = \frac{1}{3} m d_0^2 + \frac{1}{4} m \int_a^b r^2(x) dx$$

Where m is the sum of the mass of each joint and the virtual mass, and d_0 is the length of each joint. As this robot fish has six joints, therefore there is seven parts in total. The following is the calculated mass of each joint, virtual mass, and moment of inertia:

The first half of the fish $m_{\bullet} = 0.1711\text{kg}$, $m_{a\bullet} = 0.1688\text{kg}$, $I_{z\bullet} = 1.9452 \times 10^{-3} \text{kg} \cdot \text{m}^2$;

Joint 1 $m_1 = 0.0372\text{kg}$; $m_{a1} = 0.0359\text{kg}$; $I_{z1} = 2.1955 \times 10^{-5} \text{kg} \cdot \text{m}^2$;

Joint 2 $m_2 = 0.0210\text{kg}$; $m_{a2} = 0.0194\text{kg}$; $I_{z2} = 8.4153 \times 10^{-6} \text{kg} \cdot \text{m}^2$;

Joint 3 $m_3 = 0.0120\text{kg}$; $m_{a3} = 0.0104\text{kg}$; $I_{z3} = 3.4453 \times 10^{-6} \text{kg} \cdot \text{m}^2$;

Joint 4 $m_4 = 0.0065\text{kg}$; $m_{a4} = 0.054\text{kg}$; $I_{z4} = 1.3205 \times 10^{-6} \text{kg} \cdot \text{m}^2$;

Joint 5 $m_5 = 0.0039\text{kg}$; $m_{a5} = 0.0033\text{kg}$; $I_{z5} = 6.2499 \times 10^{-7} \text{kg} \cdot \text{m}^2$

Joint 6 $m_6 = 0.0050\text{kg}$; $m_{a6} = 0.0340\text{kg}$; $I_{z6} = 1.7695 \times 10^{-6} \text{kg} \cdot \text{m}^2$

Kinematical Analysis of the Robot Fish

According to the observations of the tuna fish by Donley and Sepulveda and others [3], the fish body wave equation corresponding to the swimming locomotion of this type of fish is: $h(x, t) = H(x) \sin(\omega t - kx)$, where, $h(x, t)$ is the lateral displacement of the fish. $H(x)$ is the envelope equation of the fish's swimming locomotion. ω is the swing frequency of each fish joint, k is the wave number of the fish body. $k = 5.7/l$. $H(x) = a_1 + a_2 + a_3 x^2$, Where $a_1 = 0.02l$, $a_2 = -0.12$, $a_3 = 0.3/l$.

When the frequency of each joint is 2Hz, the swing period is 0.5s. The swing cycle is divided into 10 moments. With the starting point of each joint as the center, the joint length is the intersection of the radius and the fish wave equation at that moment. The coordinate position of the six joint starting points at each moment was obtained (In this coordinate system, the front end of the fish head is the coordinate origin, the forward direction of the swimming direction is the negative direction of the x axis, and the direction of the lateral displacement is the y direction, dynamic body coordinate system). The following Table 1 is the calculated coordinates of each joint starting point at each moment.

Table 1: Coordinate position of each joint.

Unitm	Joint 1	Joint 2	Joint 3	Joint 4	Joint 5	Joint 6
t=0.1T	0.1298	0.1518	0.1692	0.1837	0.1957	0.2064
	-0.0072	-0.0058	-0.0011	0.0056	0.0129	0.0203
t=0.2T	0.1297	0.1515	0.1695	0.185	0.1977	0.2086
	-0.009	-0.0119	-0.0114	-0.0075	-0.0017	0.0053
t=0.3T	0.1298	0.151	0.1685	0.1844	0.1983	0.2105
	-0.0074	-0.0132	-0.0172	-0.0186	-0.0168	-0.0124
t=0.4T	0.13	0.151	0.1678	0.1828	0.1963	0.2092
	-0.003	-0.0096	-0.0161	-0.0217	-0.0255	-0.0268
t=0.5T	0.13	0.1516	0.1683	0.1825	0.1948	0.2064
	0.0026	-0.0024	-0.0092	-0.0165	-0.0232	-0.0291
t=0.6T	0.1298	0.1518	0.1692	0.1837	0.1957	0.2064
	0.0072	0.0058	0.0011	-0.0056	-0.0129	-0.0203
t=0.7T	0.1297	0.1515	0.1695	0.185	0.1977	0.2086
	0.009	0.0119	0.0114	0.0075	0.0017	-0.0053
t=0.8T	0.1298	0.151	0.1685	0.1844	0.1983	0.2105
	0.0074	0.0132	0.0172	0.0186	0.0168	0.0124
t=0.9T	0.13	0.151	0.1678	0.1828	0.1963	0.2092
	0.003	0.0096	0.0161	0.0217	0.0255	0.0268
t=1.0T	0.13	0.1516	0.1683	0.1825	0.1948	0.2064
	-0.0026	0.0024	0.0092	0.0165	0.0232	0.0291

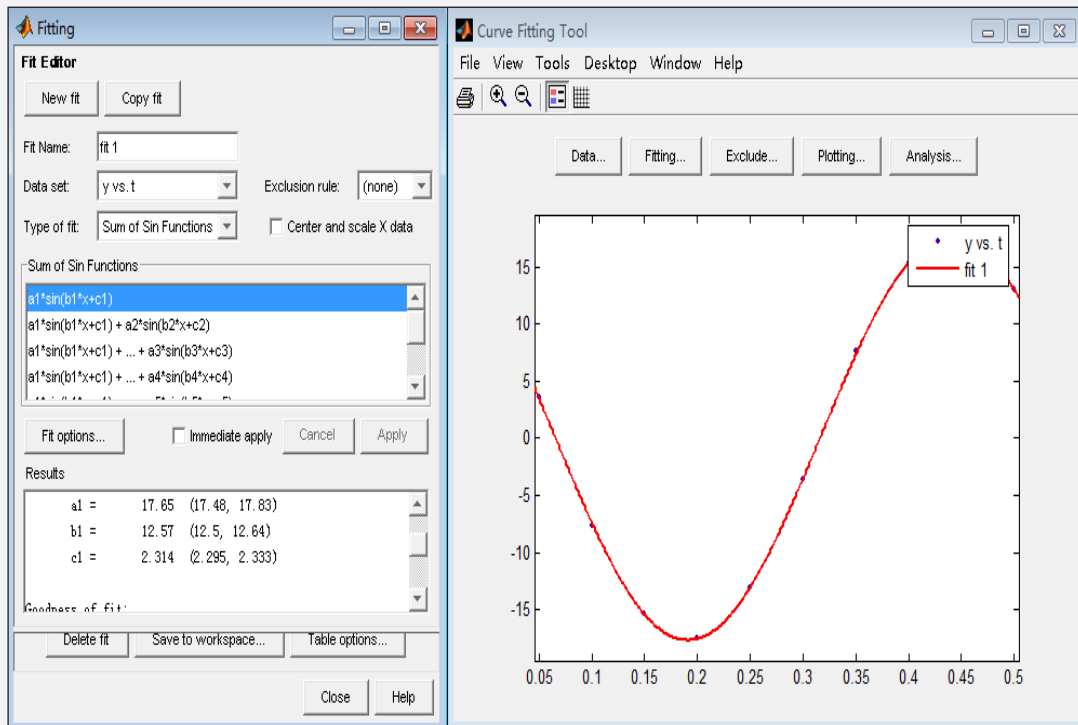


Figure 1: Fitting the movement law of each joint using Matlab cftool toolbox.

The swing movement law of each joint can be obtained by using curve fitting toolbox cftool of Matlab, As shown in Figure 1.

$$\text{Joint 1 } \theta_1 = 3.98^\circ \sin(4\pi t + 3.435)$$

$$\text{Joint 2 } y_2 = 0.0090\sin(4\pi t + 3.435); \theta_2 = 17.65^\circ \sin(4\pi t + 2.314)$$

$$\text{Joint 3 } y_3 = 0.0134\sin(4\pi t + 2.966); \theta_3 = 23.09^\circ \sin(4\pi t + 1.813)$$

$$\text{Joint 4 } y_4 = 0.0176\sin(4\pi t + 2.580); \theta_4 = 28.21^\circ \sin(4\pi t + 1.401)$$

$$\text{Joint 5 } y_5 = 0.0217\sin(4\pi t + 2.246); \theta_5 = 32.76^\circ \sin(4\pi t + 1.052)$$

$$\text{Joint 6: } y_6 = 0.0256\sin(4\pi t + 1.968) \theta_6 = 36.86^\circ \sin(4\pi t + 0.7255) .$$

Fluent Flow Field Simulation and Kinetic Analysis of Robot Fish

The Cartesian coordinate system was established: the negative direction of the x-axis was the advancing direction of the fish, the z-axis was the transverse displacement direction of the fish, and the y-axis was the longitudinal displacement direction of the fish. Ignoring the force in the y-axis direction of the fish (gravity, buoyancy, lift due to pectoral fins, and others), and considering only the x-z plane force on the body during the advancing process, the fish is only subjected to two forces: the resulting thrust due to swing water and the resistance in the forward movement.

According to the “large-amplitude elongated-body theory of fish locomotion,” the fish’s thrust is the component of the hydrodynamic force generated by the fish’s swing in the

forward direction [4]. However, due to the complexity of the flow field, there is no standard and uniform thrust formula. It is difficult to obtain relatively accurate simulation results. Therefore, the fluent flow field analysis method was used. The dynamic grid technology was used for the meshing of the fluid around a certain area of the fish, and turbulence model was used to obtain the solution. Hence, the forces exerted by the surrounding fluid on the fish body during the steady state forward movement can be obtained by simulation (surface pressure and viscous force). Further, the thrust formula can be obtained.

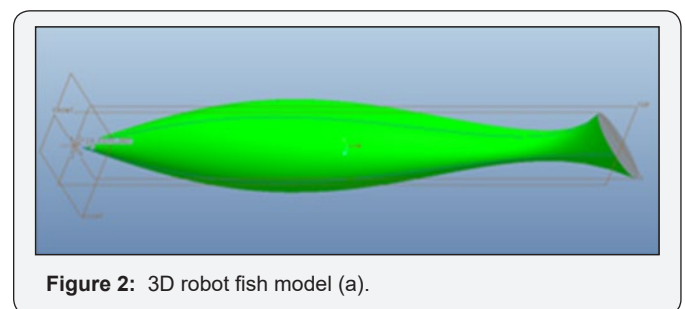


Figure 2: 3D robot fish model (a).

As shown in Figure 2a is a three-dimensional model of the extracted robot fish, Figure 2b is a plane view intercepted at $y = 0$ after the static grid division is completed. In the choice of computing domain, on the one hand, the length of the calculation area must be large enough to meet the needs of the continuous advance of the robot fish; on the other hand, the smaller calculation area can improve the calculation efficiency.

After several trials, the calculation domain was selected as rectangular, the length, width, and height were selected to be 10 times of the corresponding maximum size of the biomimetic robot fish.

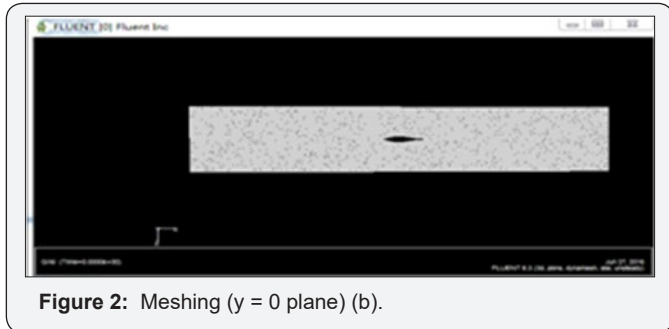


Figure 2: Meshing (y = 0 plane) (b).

In the above model, the triangular/tetrahedral mesh is used to divide the area/body domain of the region. Since the grid boundary changes with time according to the variation trend of the fish wave equation, it is necessary to define the grid as the dynamic grid in the computing domain. Also, the spring smooth method and the local mesh reconstruction method were used to ensure the quality of dynamic grid. The following is the dynamic grid parameters: the spring coefficient is 0.2, the boundary node relaxation factor is 0.4, the maximum length of the local reconstruction is 0.021, the minimum length is 0.0004, the maximum cell skew rate is 0.76, and the size function is activated, and the remaining values are default.

On the boundary condition, the boundary conditions of the six surfaces of the rectangular parallelepiped and the surfaces of the biomimetic robot fish are all non-slip condition on the wall surface, but the dynamic region is defined by the UDF (User Defined Functions) function. For the robot fish model, DEFINE-GRID-MOTION Macro was used to define the movement of fish. Take the movement at the end of the joint as an example; the custom program of this dynamic region can be defined as follows:

```
#include "udf.h"
#define PI 3.1415926
DEFINE_GRID_MOTION (guanjie6,domain,dt,time,dtime)
{
Thread *tf = DT_THREAD(dt);
face_t f;
Node *v;
real NV_VEC(omega), NV_VEC(axis), NV_VEC(dx);
real NV_VEC(origin), NV_VEC(rvec);
int n;
SET_DEFORMING_THREAD_FLAG(THREAD_T0(tf));
```

```
begin_f_loop(f,tf)
{
f_node_loop(f,tf,n)
{
v = F_NODE(f,tf,n);
if (NODE_POS_NEED_UPDATE (v))
{
NODE_POS_UPDATED(v);
NV_S(omega, =, 0.0);
NV_D[axis, =, 0.0, 1.0, 0.0];
origin[0] = 0.213;
origin[1] = NODE_Y(v);
origin[2] = 0;
omega[1]=0.2587*PI*PI*sin(4*PI*time-0.3848+PI/2);
NV_VV(rvec, =, NODE_COORD(v), -, origin);
NV_CROSS(dx, omega, rvec);
NV_S(dx, *=, dtime);
NV_V(NODE_COORD(v), +=, dx);
}
}
}
end_f_loop(f,t)
}
```

In the choice of the calculation model, because the robot fish movement belongs to the large Reynolds number movement mode, therefore the transient three-dimensional turbulence model was used for solution. Due to the wide range of applications (especially the situation of high Reynolds number), economic, reasonable accuracy, and other characteristics, k-epsilon turbulence model was used.

Since the surface of the fish is divided into seven parts according to the joint position when drawing the three-dimensional map, the force component of the wall area of the fish body in the specified direction (the advancing direction of the robot fish) can be obtained in the processing of the results.

In Table 2, $x(p)$ represents the fish surface pressure value, and $x(v)$ represents the viscous force value. It can be seen from Figure 3 and Table 2 that the positive and negative surface pressure of the fish in the z-direction is cancelled in one cycle, and the viscous force is usually in the resistance state, and its value is small relative to the surface pressure, the difference

is 2-3 orders of magnitude. Consequently, it can be neglected when fitting the thrust formula. The thrust value of each part of the fish body can be obtained as follows (N):

Fish front end: $T_0 = 0.1094\sin(4\pi t + 5.098) - 0.0410$;

Joint 1: $T_1 = 0.0875\sin(8\pi t - 0.3221) - 0.0477$;

Joint 2: $T_2 = 0.1639\sin(4\pi t + 0.9005) - 0.0835$;

Joint 3: $T_3 = 0.2328\sin(4\pi t + 0.2085) - 0.1045$;

Joint 4: $T_4 = 0.2410\sin(4\pi t - 0.3612) - 0.1170$;

Joint 5: $T_5 = 0.2247\sin(4\pi t + 5.575) - 0.1360$;

Joint 6: $T_6 = 1.638\sin(8\pi t + 1.881) - 1.571$.

The influence of viscous resistance (frictional resistance) is small and negligible in the case of fish swimming locomotion that has a large Reynolds number (As demonstrated in Table 2). The pressure resistance, which played a major role, can be calculated by the standard Newton equation [5]:

Table 2: Force values of various parts of the fish (x direction).

Unit:N	Fish front end	Joint 1	Joint 2	Joint 3	Joint 4	Joint 5	Joint 6
t=0.1T							
x(p)	1.95E-02	6.97E-02	6.50E-02	2.13E-02	-2.24E-02	-4.94E-02	6.17E-03
x(v)	1.83E-05	-2.05E-04	7.08E-05	3.10E-04	3.22E-04	1.91E-04	-9.12E-04
t=0.2T							
x(p)	-2.22E-02	5.17E-02	1.21E-01	1.24E-01	5.88E-02	-2.56E-02	-1.85E+00
x(v)	6.42E-04	-6.36E-05	-1.19E-04	1.89E-04	4.63E-04	4.23E-04	4.57E-03
t=0.3T							
x(p)	-4.57E-02	-6.32E-02	2.89E-02	1.18E-01	1.40E-01	9.96E-02	-2.71E+00
x(v)	1.20E-03	5.37E-04	1.76E-04	2.83E-04	5.98E-04	7.33E-04	1.15E-02
t=0.4T							
x(p)	3.55E-02	-1.65E-01	-1.66E-01	-7.01E-02	2.95E-02	1.01E-01	-4.74E-01
x(v)	1.56E-03	1.37E-03	7.60E-04	3.78E-04	3.97E-04	6.39E-04	1.58E-02
t=0.5T							
x(p)	1.30E-01	-1.05E-01	-2.88E-01	-2.82E-01	-1.83E-01	-1.01E-01	7.99E-01
x(v)	1.47E-03	1.56E-03	1.46E-03	7.45E-04	2.79E-04	2.18E-04	3.34E-03
t=0.6T							
x(p)	6.10E-02	-1.21E-02	-2.48E-01	-3.75E-01	-3.39E-01	-2.79E-01	-1.62E+00
x(v)	1.67E-03	1.18E-03	1.59E-03	1.09E-03	4.30E-04	1.84E-04	2.98E-03
t=0.7T							
x(p)	-1.08E-01	1.14E-02	-9.27E-02	-2.90E-01	-3.74E-01	-3.73E-01	-3.30E+00
x(v)	1.95E-03	8.66E-04	1.35E-03	1.49E-03	1.03E-03	1.07E-03	9.32E-03
t=0.8T							
x(p)	-2.12E-01	-6.87E-02	7.66E-04	-8.91E-02	-2.27E-01	-3.18E-01	-3.94E+00
x(v)	1.91E-03	6.14E-04	7.10E-04	1.12E-03	1.17E-03	1.07E-03	9.32E-03
t=0.9T							
x(p)	-1.57E-01	-9.34E-02	-5.09E-03	2.14E-02	-3.51E-02	-1.28E-01	-3.17E+00
x(v)	1.57E-03	4.38E-04	2.59E-04	5.49E-04	7.77E-04	8.31E-04	1.04E-02
t=1.0T							
x(p)	-8.34E-02	-7.31E-02	-9.68E-03	3.99E-02	4.06E-02	1.00E-02	-1.44E+00
x(v)	1.23E-03	3.13E-04	1.20E-04	2.47E-04	5.27E-04	6.31E-04	7.81E-03
t=1.1T							
x(p)	-8.60E-03	8.76E-04	5.16E-02	7.90E-02	6.02E-02	2.87E-02	2.19E-01
x(v)	1.22E-03	1.47E-02	1.04E-04	2.24E-04	4.63E-04	6.16E-04	3.12E-03
t=1.2T							
x(p)	3.09E-02	2.54E-02	1.10E-01	1.66E-01	1.35E-01	5.94E-02	-6.56E-01
x(v)	1.64E-03	7.49E-04	3.95E-04	4.55E-04	6.65E-04	7.34E-04	8.08E-03

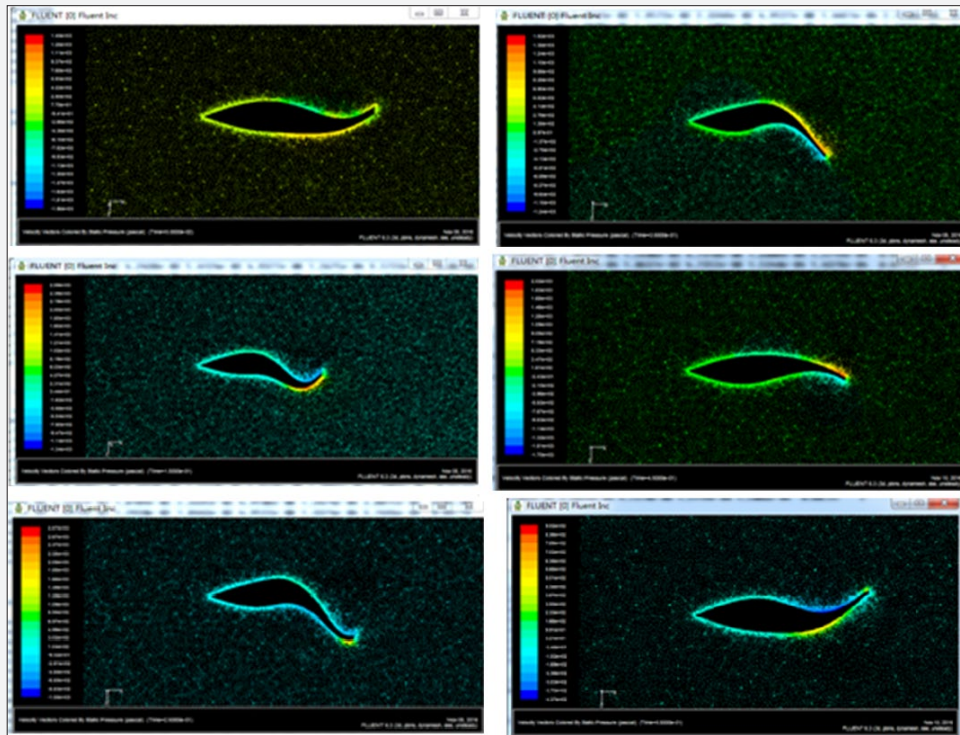


Figure 3: The fish body surface pressure changes during a cycle.

$$D_p = 0.5C_p S_p U^2 \rho$$

Where C_p is the resistance coefficient, usually 1.2; S_p is the effective area, in the practical application (is the displacement) can be used as the effective area of action as the fish moves in the water, because the density of fish and water are basically the same, $S_p = (m / \rho)^{2/3}$ [6]. U is the average speed of swimming locomotion; ρ is the density of water.

It can be concluded that the rear joint (caudal fin) provides the maximum thrust, accounting for more than 80% of the total thrust, so the caudal fin drive mode is selected; electromagnetic drive has advantages of compact structure, pollution-free, high reliability, and large driving force, and accurate process control can be achieved. The cyclic oscillation-driving mode is selected to be the electromagnetic drive.

Table 3: Basic components required for the simulation circuit.

Equipment	MCU	Oscilloscope	DAC Converter	Polarity Converter	Power Source	Crystal Resonator
Model	8051single-chip microcomputer	Dual oscilloscope	8-bit voltage DAC	Adder circuit	Vcc, Vdd, Vee, GND	HC-49/U_11MHz

Simulation circuit has been completed. A waveform generator and an oscilloscope were used as waveform generation and acquisition circuit (sinusoidal wave as an example) in Multisim. The amplitude was set to 255V, the cycle was 1s, as shown in Figure 4 & 5.

Research on Control Signal of Electromagnetic Drive Robot Fish

Signal transformation

The standard electromagnetic coil current waveform was digitized, and then through the MCU processing the signal was transferred to the DAC module for digital-analog transformation to reproduce the analog control signal. The realization of the control signal was the acquisition, storage, and reproduction of the standard control waveform, which was used to drive the electromagnetic coil that further drove the caudal fin movement. The basic flow of the control drive circuit is shown in Figure 4. The components used in the Multisim simulation are described in Table 3.

After the standard sine wave was obtained, the collection and digital discretization was required. As shown in Figure 6, the oscilloscope in Multisim provided the function of waveform sampling. Click "Save" on the oscilloscope in the figure, the settings of the sampling time interval and number of sampling points of the oscilloscope will be displayed. To ensure signal

accuracy, 120 points were sampled in a cycle. The sampled data was set as a binary output text file.

After the sampling data was obtained, start the single-chip microcomputer-programming interface of the completed

circuit simulation platform. The collected discrete value's output was through the single-chip microcomputer one by one cyclically. The programming interface and the program are shown in Figure 7.

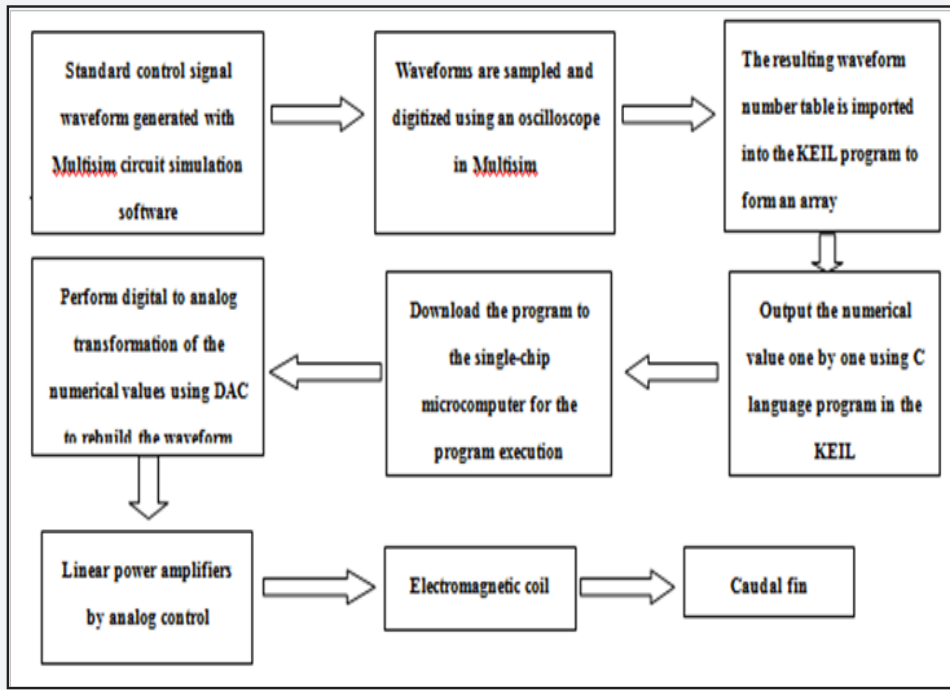


Figure 4 : The basic flow diagram of the control drive circuit.

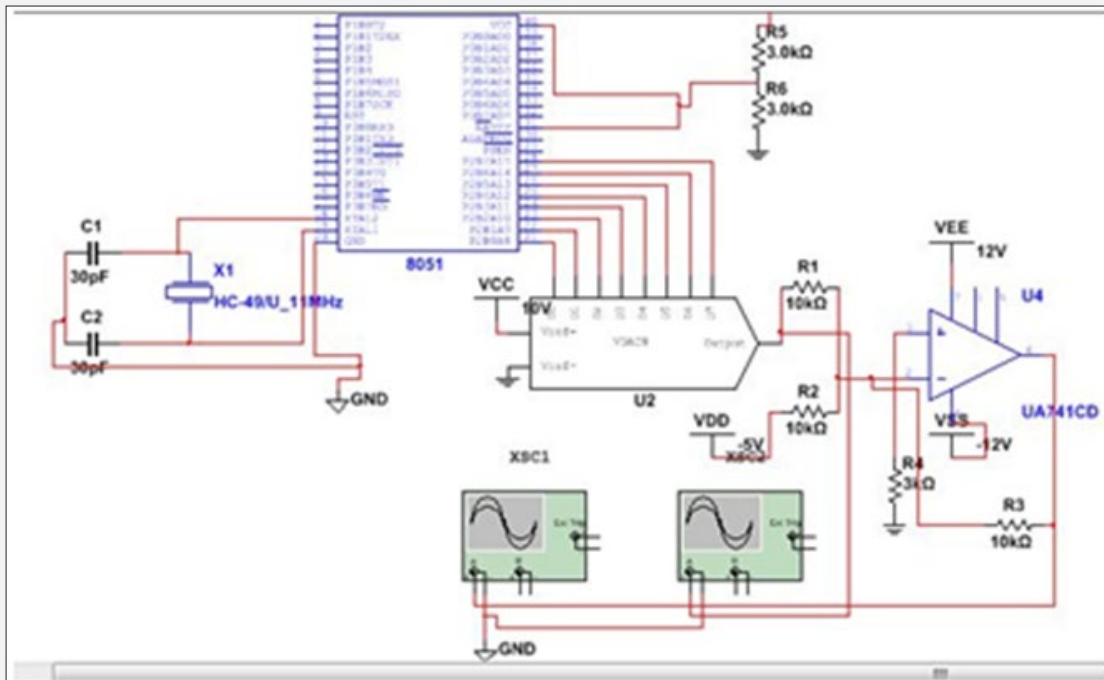


Figure 5 : Thows the circuit simulation diagram.

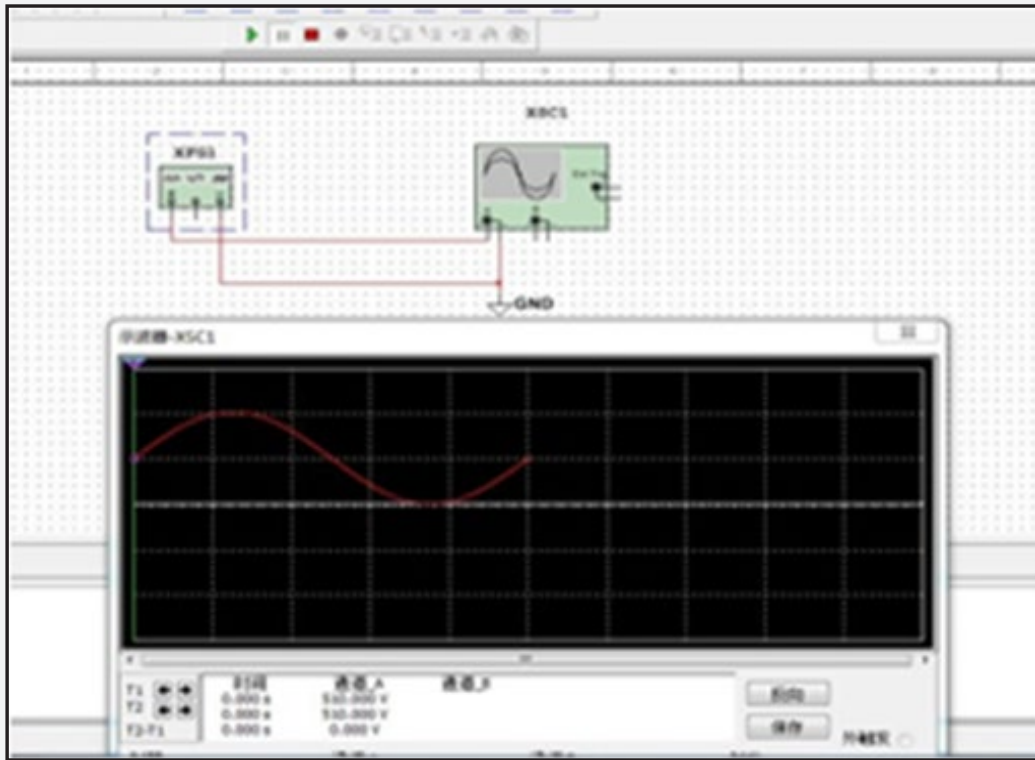


Figure 6 : Generation and acquisition of the control waveform.

```

#include<8051.h>
#include<math.h>
void delay(int m);
void main()
{
    unsigned int zx[120]={128, 134, 141, 147, 154, 160, 173, 179, 185, 191, 197, 202, 208, 213, 218, 222, 227, 231, 234, 238,
    241, 244, 247, 249, 251, 252, 253, 254, 255, 254, 255, 254, 253, 252, 251, 249, 247, 244, 241, 238,
    234, 231, 227, 222, 218, 213, 208, 202, 197, 191, 185, 179, 173, 167, 161, 154, 147, 141, 134, 128,
    121, 114, 108, 101, 95, 88, 82, 76, 70, 64, 58, 53, 47, 42, 37, 33, 28, 24, 21, 17,
    14, 11, 8, 6, 4, 3, 2, 1, 0, 1, 0, 1, 2, 3, 4, 6, 8, 11, 14, 17,
    21, 24, 28, 33, 37, 42, 47, 53, 58, 64, 70, 76, 82, 88, 94, 100, 108, 114, 121, 127};

    int i;
    while(1)
    {
        for(i=0;i<120;i++)
        {
            P2=zx[i];
            delay(5);
        }
    }
}

void delay(int m)
{
    int k;
    for(k=0;k<m;k++);
}
    
```

Figure 7 : Simulation program.

After programming, the program is successfully downloaded to the single-chip microcomputer, click on the “start simulation,” back to Figure 5 interface and open the two

oscilloscopes in the figure, waveform as shown in Figure 8 can be observed (Figure 9).

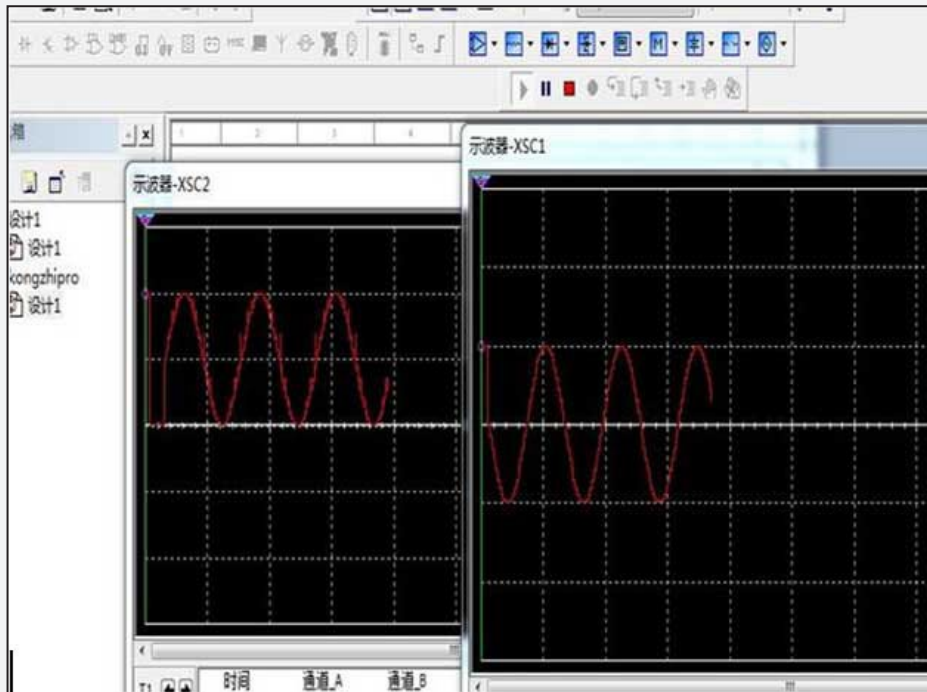


Figure 8 : waveform displayed by the oscilloscope.

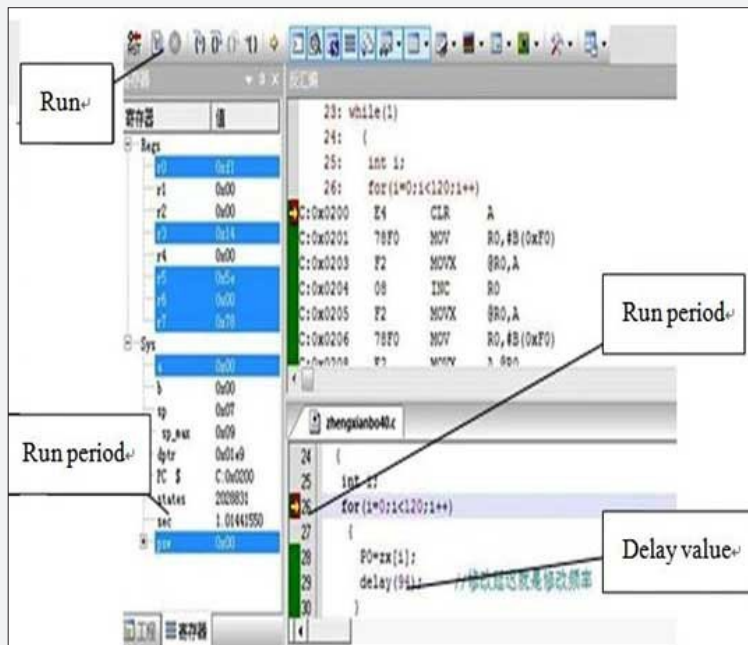


Figure 9 : Keil frequency debugging.

Oscilloscope XSC2 displays the 8-bit DAC direct output of the control signal; the oscilloscope XSC1 displays the output control signal of the DAC output after passing through the polarity converter. For the frequency of the waveform, delay value in the parentheses of the delay statement in the program can be adjusted. When calling the delay program, the single-chip microcomputer will adjust the output hold time of each

digit according to the delay value in parentheses, and thus the frequency of the whole waveform can be adjusted. The amplitude needs to be matched based on the characteristics of the power amplifier module in the actual circuit and the DAC module in the actual circuit has a reference voltage setting [7-10].

The simulation program as shown in Figure 3 & 4 was then transplanted to the Keil single-chip microcomputer programming software. After the program was successfully compiled, the crystal resonator frequency was set to be the crystal resonating frequency of the single-chip microcomputer, which was 12Mhz. The Keil debugging interface was started, break points out of the cycles were set, and the delay parameter in the brackets of the “delay ()” statement was adjusted continuously until the output cycle reached 1s, namely, control signal so that the caudal fin swing cycle was 1Hz. The debugging interface of Keil as shown in Figure 4 & 5 was entered. In every click of “run”, the program executed a cycle, and “sec” increased accordingly, and the added value was the time required to output a complete waveform [11-14].

After debugging, the program was downloaded to the

single-chip microcomputer. The DAC output control waveform can be observed by connecting the DAC module output with the oscilloscope. It can be seen that the actual circuit output control signal and the simulation circuit output signal were exactly the same.

Signal adjustment

The DAC module was connected with the STC89C52 development board with the downloaded test program. The output of the DAC module was connected to the input of the power amplifier module. The DAC module and the power amplifier module shared the DC ± 15V power supply. The overall circuit of the control platform is shown in Figure 10. The “delay ()” delay parameter was modified in the Keil programming debugging interface, the signal frequency was the electromagnetic coil operating frequency.



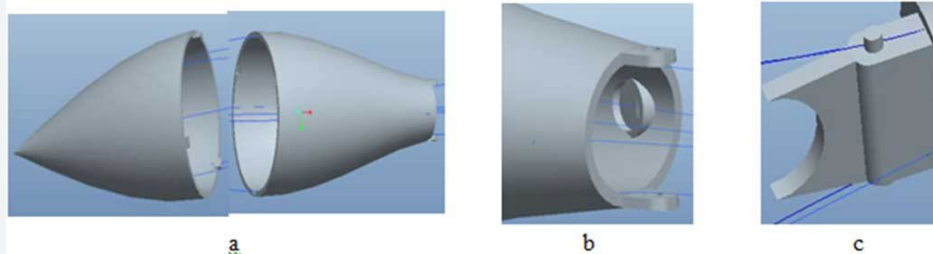
Figure 10 : Photo of the electromagnetic servo control circuit.

Experimental Study

Development of experimental prototype of robot fish

The external fish body shape curve was imported into the Pro/E three-dimensional modelling software; closed fish surface shape can be obtained by the use of “variable cross-

section scanning” tool. Then, “thickening” operation was performed on the surface, with the set thickness of 1.8mm. The closed fish body shell was thus obtained. Considering the fish body assembly, weight allocation, fish body was designed into a removable form, as shown in Figure 11.



- a Fish body design of the robot fish.
- b Permanent magnet slot design.
- c Electromagnetic coil mounting bracket design.

Figure 11: Three-dimensional structural design of each part of the robot fish.

After modeling, the fish body model was obtained with the use of precision 3D printing, the printing material was resin. The polypropylene caudal fins were tailored to thin caudal fins according to the caudal fins of the actual tuna fish, and the flexible caudal fins were then fixed on the connecting parts as shown in Figure 12. Underwater experiments are shown in Figure 13.



Figure 12: Polypropylene caudal fin.

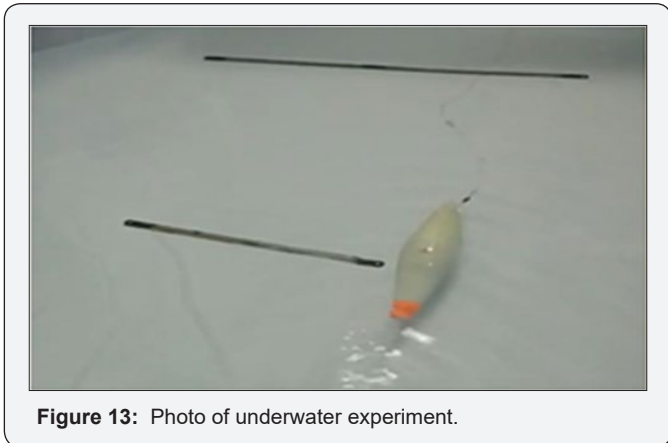


Figure 13: Photo of underwater experiment.

Electromagnetic drive robot fish underwater experiment

Fish body linear curve swimming experiment: In the experiment, the swing frequency of the fish when swimming along straight lines is set within 1-8Hz. The amplitude of the drive voltage is set between 2-6V. After adjustment of the fish

weight, the control signal waveform acquisition was used to generate 1-8Hz sinusoidal signal, the signal waveform are shown in Figure 14. By adjusting the frequency of the control signal through adjusting the delay time of the sinusoidal output program, the obtained experimental data is recorded in Table 4, the distribution diagram of velocity - frequency under different voltage amplitude is shown in Figure 15.

The above data is shown in Figure 15. The greater the amplitude of the driving voltage signal, the faster the fish swims. At different drive voltage amplitude, the best swing frequency was basically the same; at about 2Hz, the fastest swimming speed was achieved. As the high drive voltage heats up the coil, it is desirable to operate at low voltage, hence at 2V voltage, 2Hz, the swimming speed of 81.74mm/s was selected as the best electromagnetic drive control signal [15-18].

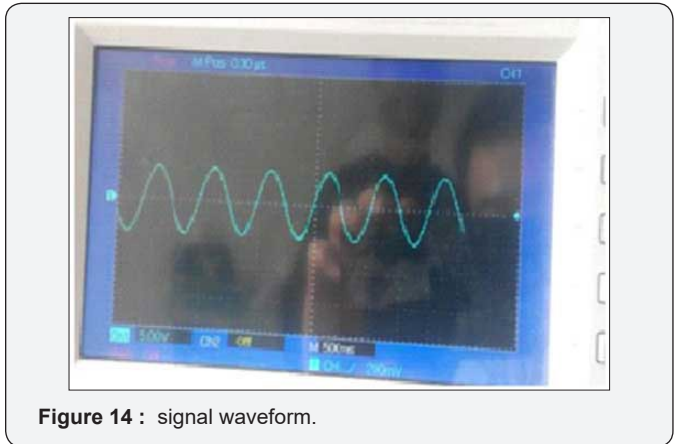


Figure 14 : signal waveform.

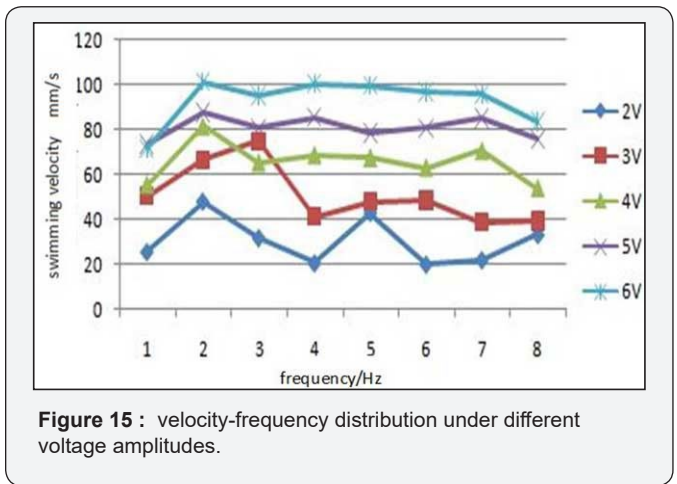


Figure 15 : velocity-frequency distribution under different voltage amplitudes.

Table 4: Swimming experiment data.

Frequency	2	3	4	5	6
1	25.59	50.20	55.49	73.53	71.74
2	48.02	66.40	81.74	87.77	101.48

3	31.85	74.82	65.42	80.69	95.42
4	20.60	40.96	68.87	85.62	100.87
5	43.12	47.97	67.60	78.70	100.07
6	20.07	48.39	63.13	80.69	97.15
7	22.02	38.74	70.75	85.03	96.03
8	33.22	39.16	53.86	75.72	83.80

Conclusion

Based on the actual physical appearance of the tuna and the wave equation derived from observing its swimming locomotion, the motion law of each joint of the robot fish is obtained through the discrete fitting method, and the motion law is utilized as the basis of the control signal of the electromagnetically driven robot fish. With the utilization of the fluent flow field analysis software, a dynamic grid technique was used to mesh the fluid around the fish body. By analyzing the surface pressure value of the simulated fish body in the steady state of forward movement, the thrust values of each part of the fish body were obtained. Hence, the electromagnetic-driven caudal fin robot fish was determined as the optimal design. Based on the idea of digital-analog conversion, the drive control signal waveform was first digitally discretized. Then, it was converted through the C51 single-chip microcomputer and DAC digital-to-analog converter. Finally, the simulated amplified analog output was obtained through the OPA544 op amp chip in accordance with the waveform of the control signal. Electromagnetic coil drive signal with variable frequency and voltage was thus achieved. An electromagnetic driven caudal fin robot fish prototype was successfully produced, a number of robot fish underwater experiments were designed, and a series of experimental data was obtained. Based on the linear swimming experiment of the robot fish prototype, it was obtained that the optimal value of the electromagnetic drive signal is 2V, 2HZ when the electromagnetic driven caudal fin robot fish was at a relatively high speed. Based on this, the next steps of the study lays on the following two aspects:

1. Apply the electromagnetic coil control theory to the underwater experiments of robot fish; produce new robot fish prototype;
2. Build functional platforms on the bases of the existing robot fish platform, so that the robot can achieve obstacle avoidance, tracking, information transmission, and other intelligent functions, and fully demonstrate the unique advantage of biomimetic robot fish as underwater vehicles.

References

1. Zhikun C (2008) Simulation and experimental study on the flexible spine of robot fish. Harbin Institute of Technology (Natural Science Edition), Harbin.

2. Hong C (2006) Study on the Motion Mechanism of Cruise and Maneuvering of Biomimetic Robot Fish. University of Science and Technology of China, Hefei.
3. JM Donley, Epulveda CAS, Konstantinidis P (2004) Convergent Evolution in Mechanical Design of Lamnid Sharks and Tunas. *Letters to Nature* 429: 61-65.
4. Zuo C (2013) Design and experimental study of swing drive flexible robot fish. Harbin Institute of Technology, Harbin.
5. Yaohui Y (2014) Research on the robot fish for mine flooding accident detection. China University of Mining and Technology, Beijing.
6. Chunzhao G (2007) Optimization design and simulation of virtual fish-mimetic robot based on the fish body muscle model. University of Science and Technology of China, Hefei.
7. Yingxiang L (2007) Two joint robot fish body and dynamics research. Harbin Institute of Technology, Harbin.
8. Qian W (2009) Dynamic analysis of three-joint robot fish without lift potential swimming. Xi'an University of Technology, Xi'an.
9. Shuxin Z, Qingsong H (2013) Three-dimensional modeling of carp and numerical calculation of flow field force. *Journal of Shanghai Ocean University* 22(6): 855-861.
10. Guan Z, Gao W, Gu N (2010) 3D Hydrodynamic Analysis of a Biomimetic Robot Fish: Control, Automation, Robotics, and Vision. Singapore, pp. 793-798.
11. Park HC, Lee E, Choi HS (2013) Application of FSI (Fluid Structure Interaction) to Biomimetic Robot Fish: International Conference on Ubiquitous Robots and Ambient Intelligence (URAI). Ramada Plaza Jeju Hotel, Jeju, Korea, pp. 439-441.
12. Yadong H, Weijie Z, Shengkuan Y (2014) Design and magnetic circuit calculation of electromagnetic steering gear for underwater vehicle. *Water Warfare and Ship Protection* 22 (1): 49-51.
13. Shumeng L, Bin L, Zhiyuan L (2011) Design and experimental study of driving coil of coil drivers. *Foreign Electronic Measurement Technology* 30 (8): 54-57.
14. Xiaome D (2006) Research on a number of technical issues of miniature electromagnetic driver. Tianjin University, Tianjin.
15. Guangming X, Chenguang H (2013) Autonomous biomimetic robot fish. Harbin Engineering University Press, Harbin, pp. 22-40
16. Weiwei S (2009) Study and design of caudal fin propulsion system for biomimetic robot fish. Yanshan University, Hebei.
17. Wenguang W (2010) Experimental study on the propulsion performance of the biomimetic tuna robot fish. China University of Science and Technology, Anhui.
18. Chang L (2007) Study on modeling and control method of caudal fin robot fish. Harbin Institute of Technology, Harbin, p. 2.



This work is licensed under Creative Commons Attribution 4.0 License
DOI: [10.19080/RAEJ.2018.02.555587](https://doi.org/10.19080/RAEJ.2018.02.555587)

**Your next submission with Juniper Publishers
will reach you the below assets**

- Quality Editorial service
- Swift Peer Review
- Reprints availability
- E-prints Service
- Manuscript Podcast for convenient understanding
- Global attainment for your research
- Manuscript accessibility in different formats
(Pdf, E-pub, Full Text, Audio)
- Unceasing customer service

Track the below URL for one-step submission
<https://juniperpublishers.com/online-submission.php>